Bioorganic Chemistry 99 (2020) 103584

Contents lists available at ScienceDirect

Bioorganic Chemistry

journal homepage: www.elsevier.com/locate/bioorg

Synthesis, anti-convulsant activity and molecular docking study of novel thiazole pyridazinone hybrid analogues

Aness Ahmad Siddiqui[a,*], Sangh Partap[a], Subuhi Khisal[a], Mohammad Shahar Yar[a], Ravinesh Mishra[b]

[a] Department of Pharmaceutical Chemistry, School of Pharmaceutical Education and Research, Jamia Hamdard University, New Delhi, India
[b] School of Pharmacy and Emerging Sciences, Baddi University of Emerging Sciences & Technology, Baddi (Solan), Himachal Pradesh 173205, India

ARTICLE INFO

Keywords:
Thiazole
Pyridazinone
Anticonvulsant activity
Pharmacophore based drug design
GABA

ABSTRACT

Pyridazinone analogues have been known to be potential candidates for anticonvulsant agents. We have identified several pyridazinone-based anticonvulsant agents. As a continuation to our previous research, a series of hybrid pyridazinone-thiazole connected through amide linkage were designed and synthesized. Among these, compound SP-5F demonstrated significant anticonvulsant activity with median effective dose of 24.38 mg/kg (MES) and 88.23 mg/kg (scPTz). Results of GABA estimation showed a marked increase in the GABA level when compared with control. Molecular docking studies at the active site of GABA receptor, further confirmed the GABA modulatory effects of SP-5F.

1. Introduction

Epilepsy is very dangerous CNS diseases due to hyper synchronous electrical discharge in neurons. Globally, around fifty million people are suffering from this destructive neurological condition and out of these, ninety percent patients are from developing countries [1,2]. Moreover, the risk of seizure, trauma, hospitalization and mortality is very high in epileptic patients which have very strong negative impact on patient's physical, mental and social health [3]. Although, several newer classes of antiepileptic drugs (AEDs) have emerged in the past 15 years, but complete treatment of epilepsy is still a long way [4,5]. Moreover, these AEDs are ineffective against the 30% refractory epileptic patients and possess severe side effects such as, neurotoxicity, anemia, hepatic failure etc. [6]. Thus, there is always a constant need to develop newer effective anticonvulsant agent with minimal side-effects (see Fig. 1).

Pyridazinone is an attractive lead for anticonvulsants, is a cyclized derivative of β-aroylpropionic acid which contain GABA like pharmacophore [7]. Several pyridazinone derivatives have been reported to possess seizure protective activity in number of animal models [8]. Moreover, designing of anticonvulsant agents based on pharmacophoric pattern has received much attention in the AED discovery. Based on these, several newer anticonvulsant agents have been described previously that demonstrated significant *in vivo* and *in vitro* binding and receptor-mediated seizure protective activity [9–11]. In previous manuscript, we detailed our efforts to identify hybrid pyridazinone analogues as anticonvulsant agents. These compounds were found to be safer and effective anticonvulsant agents having GABA modulatory effects [12]. Subsequently, an attempt has also been made for hit-to-lead optimization of pyridazinoneanalogues by introducing amide linkage as hydrogen bonding domain between the two lipophilic nuclei. Results revealed that some of these derivatives demonstrated admirable *in vitro*GABA-ATinhibition. However, the partition coefficient of these derivatives was found to be higher (log$P$ > 5) which conceivably contributed to their high neurotoxicity [13]. Encouraged by these observations and in continuation of our research program [14], it was of interest to further optimize pyridazinone analogues by the modification the lipophilic domain which resulted into optimal lipophilic derivatives.

2. Result and discussion

2.1. Chemistry

In the first step, β-aroyl propionic acids (SP-1a to SP-19a) were synthesized by Lewis acid-catalyzed Friedel-Crafts acylation of appropriate hydrocarbon with succinic anhydride [15]. Further, condensation of the same (SP1a-SP19a) with hydrazine hydrate afforded

* Corresponding author at: Department of Pharmaceutical Chemistry, School of Pharmaceutical, Education and Research, Jamia Hamdard, New Delhi 110062, India.
E-mail address: anees_asiddiqui@rediffmail.com (A.A. Siddiqui).

https://doi.org/10.1016/j.bioorg.2020.103584
Received 20 October 2019; Received in revised form 6 December 2019; Accepted 12 January 2020
Available online 27 January 2020
0045-2068/

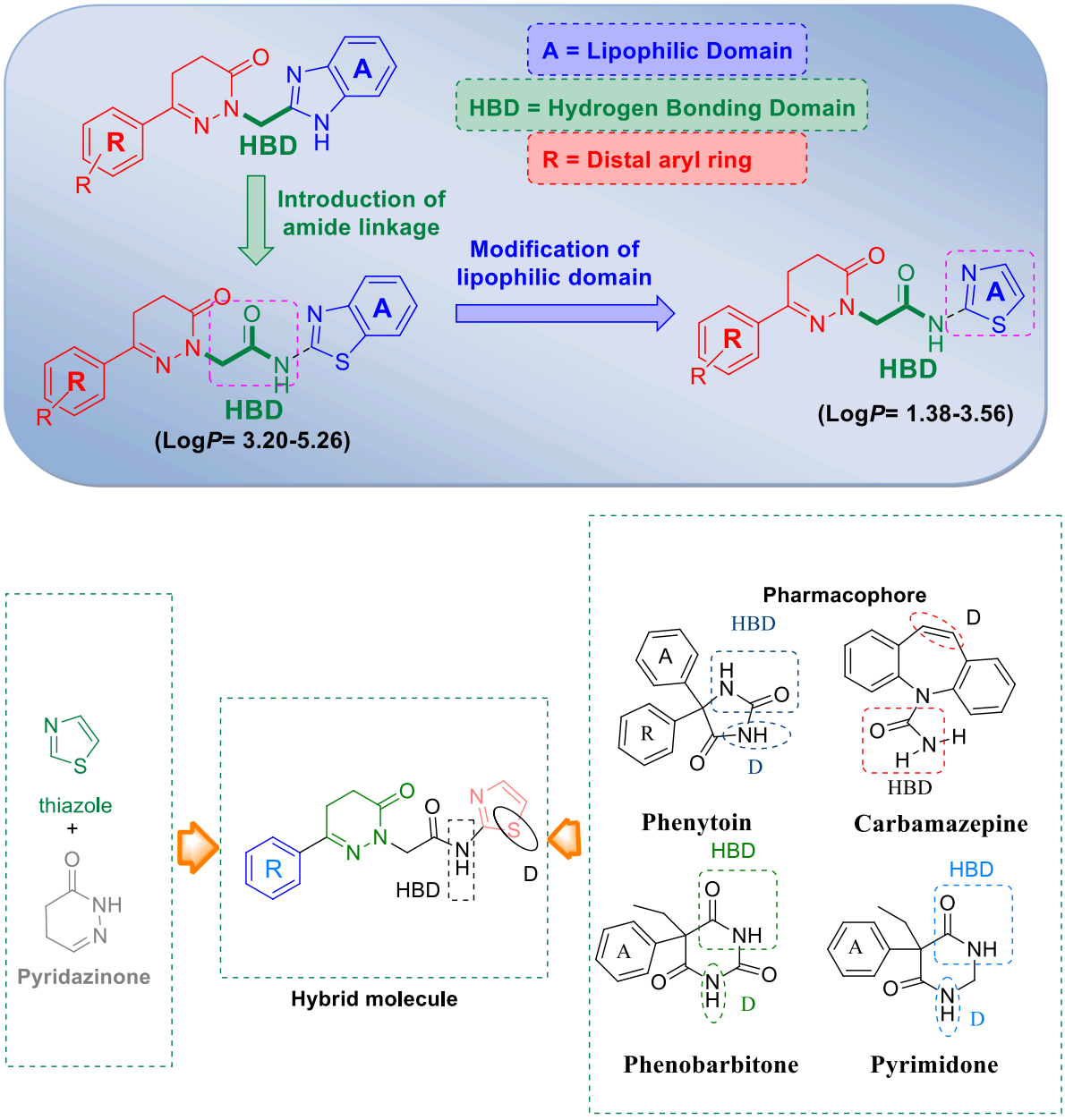

Fig. 1. Lead optimization of anticonvulsant pyridazinones.

different 6-substitued-4,5-dihydropyridazine-3(2H)-one (SP1b-SP18b) in the second step [16]. The synthetic route of synthesized derivatives is outlined in Scheme 1. Subsequently, 6-substitued-4,5-dihydropyridazine-3(2H)-one on treatment with 2-chloro-N-(thiazol-2-yl)acetamide in the presence of potassium carbonate in dry DMF produce substituted phenyl-5,6-dihydropyridazin-1(4H)-yl)-*N*-(thiazol-2-yl) acetamide(SP1F-SP18F). The synthetic route of synthesized derivatives is outlined in Scheme 1.

The completion of reactions and purity of synthesized compounds was confirmed by TLC using ethyl acetate: hexane (4:6) as solvent system and melting points were recorded. The structures were characterized on the basis of elemental and spectral data analyses. The SP-5F recorded IR spectra in the range of 1640 and 3410 cm^{-1} which shows the appearance of C=O and N−H absorption bands respectively. A broad singlet proton signal (-NHD_2O exchangeable) was shown by H^1-NMR spectra at δ 9.32 ppm. SP-5F having methylene proton displayed a characteristic singlet signal at δ 3.92 ppm and the triplet peaks at δ 3.62& 2.42 ppm confirmed the pyridazinone proton. Compound SP-5F with ^{13}C NMR spectra as a prototype revealed two up-field peaks at δ 54.12 ppm of methylene carbons and the carbonyl carbon appeared downfield at δ 168.29 ppm.

2.2. Pharmacology

All the synthesized compounds were evaluated for maximal electroshock seizure (MES) and subcutaneous pentylenetetrazole (scPTZ) tests. The compounds were administered intraperitoneally (*ip*) in-different doses of 30,100 and 300 mg/kg and end points were recorded at two different time intervals of 0.5 h and 4 h, respectively. Neurotoxicity of the synthesized compounds was evaluated by rotarod method. Results of anticonvulsant screenings along with neurotoxicity studies were summarized in Table 2.

In the preliminary MES screening, all the compounds showed some degree of protection which is clear indicative that these pyridazinone analogues have potential to control seizure effective. Among the eighteen compounds tested in MES, compound **SP-5F**having *p*-chlorophenyl

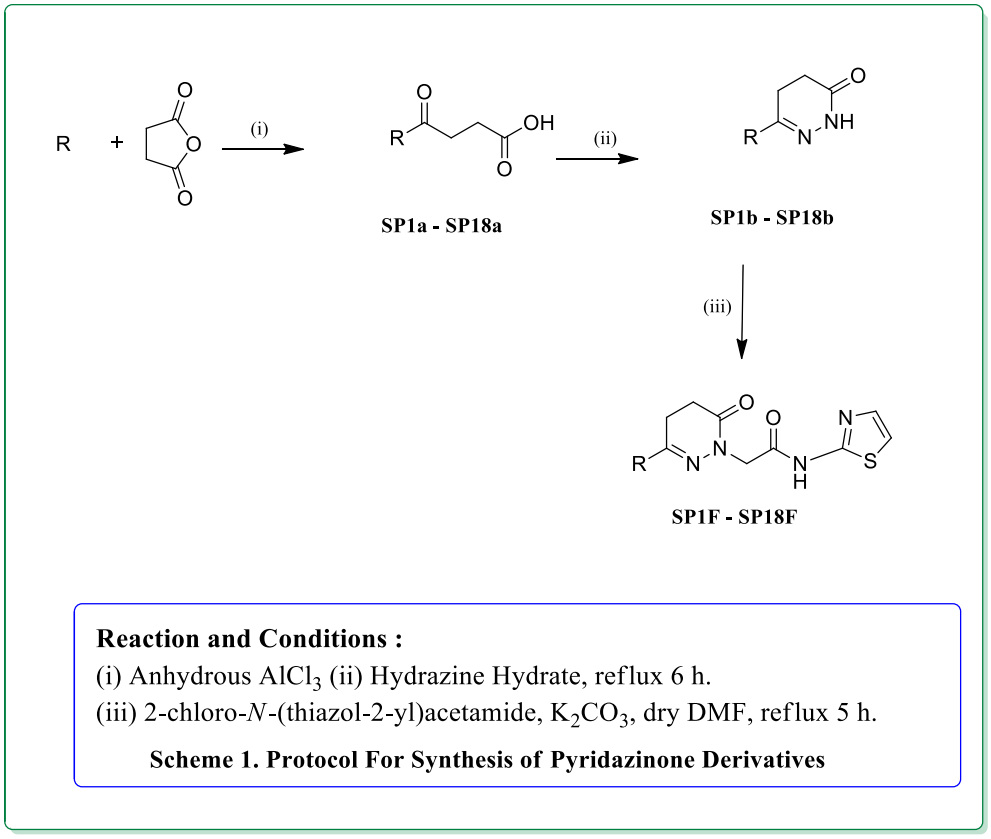

Scheme 1. Synthesis route to the synthesized title compound SP (1a-18a) to SP (1F- 18F).

substitution prevented the hind limb tonic extension (HLTE) after 0.5 and 4 h at the lower dose of 30 mg/kg against the 50 mA electroshock. Thus, compound **SP-5F** (LogP 2.03) emerged as the most effective anticonvulsant having rapid onset and longer duration of action. At the same dose of 30 mg/kg, compound **SP-17F** (LogP 2.31) having *p*-bromophenyl substitution also provided protection against HLTE with rapid onset and short duration of action however, at higher dose of 100 mg/kg showed protection at longer duration. Compound **SP-12F** (LogP 2.59) having dicholorophenyl group showed protection at a dose of 100 mg/kg after 0.5 and 4 h. Rest of the compounds showed protection only at highest dose (> 300 mg/kg).

The compounds which were found active during MES test were further screened for scPTZ test. The ScPTZ is a confirmatory screening test for the compounds to be active against the absence seizure. In

Table 1

Physicochemical parameters of the title compounds (SP-1F to SP-18F).

Compound	R	(SP-1F to SP-18F)					
		Mol. Formula	Mol. Weight	M.P. (°C)	R_f[a]	% Yield	Log P[b]
SP-1F	Phenyl	$C_{15}H_{14}N_4O_2S$	314.36	189–191	0.48	46	1.48
SP-2F	*p*-Fluro-phenyl	$C_{15}H_{13}N_4O_2S$	332.35	238–242	0.64	57	1.63
SP-3F	*p*-Tolyl	$C_{16}H_{16}N_4O_2S$	328.39	270–272	0.76	73	1.96
SP-4F	*p*-Anisyl	$C_{16}H_{16}N_4O_3S$	344.39	218–220	0.55	38	1.35
SP-5F	*p*-Chloro-phenyl	$C_{15}H_{13}ClN_4O_2S$	348.81	262–264	0.61	**68**	**2.03**
SP-6F	*p*-Ethyl phenyl	$C_{17}H_{18}N_4O_2S$	342.42	298–300	0.42	60	2.45
SP-7F	3,4-Dimethylphenyl	$C_{17}H_{18}N_4O_2S$	342.42	258–260	0.68	44	2.45
SP-8F	2,5-Dimethylphenyl	$C_{17}H_{18}N_4O_2S$	342.42	248–250	0.51	59	2.45
SP-9F	2,4-Dimethylphenyl	$C_{17}H_{18}N_4O_2S$	342.42	254–256	0.48	58	2.45
SP-10F	*p*-Isobutyl phenyl	$C_{19}H_{22}N_4O_2S$	370.47	290–292	0.72	47	3.13
SP-11F	Naphthyl	$C_{19}H_{16}N_4O_2S$	364.42	268–270	0.57	63	2.47
SP-12F	3,4-Dichloro-phenyl	$C_{15}H_{12}Cl_2N_4O_2S$	383.25	178–180	0.62	70	2.59
SP-13F	*p*-Benzyl phenyl	$C_{22}H_{20}N_4O_2S$	404.48	201–203	0.48	40	3.57
SP-14F	*p*-Phenoxy phenyl	$C_{21}H_{18}N_4O_3S$	406.46	229–231	0.71	56	3.01
SP-15F	*p*- Propyl phenyl	$C_{18}H_{20}N_4O_2S$	356.44	287–289	0.58	38	2.80
SP-16F	*p*-Biphenyl	$C_{21}H_{18}N_4O_2S$	390.46	244–246	0.76	32	3.15
SP-17F	*p*-Bromo-phenyl	$C_{15}H_{13}BrN_4O_2S$	393.26	169–171	0.68	61	2.31
SP-18F	2-Thienyl	$C_{13}H_{12}N_4O_2S_2$	320.39	195–197	0.56	49	1.46

[a] Solvent system- Ethyl acetate: Hexane (4:6).
[b] Log P was determined by octanol: phosphate buffer method.

Table 2
Anticonvulsant activity and minimal motor impairment of the synthesized compounds (SP-1F to SP-18F).

Compound	Intraperitoneal injection in mice					
	MES screen		scPTZ screen		Neurotoxicity screen	
	0.5 h	4 h	0.5 h	4 h	0.5 h	4 h
SP-1F	300	–	–	–	X	X
SP-2F	100	300	100	300	–	–
SP-3F	300	–	300	–	X	X
SP-4F	300	–	300	–	X	X
SP-5F	30	30	100	100	–	–
SP-6F	100	300	300	X	–	–
SP-7F	300	X	300	X	–	–
SP-8F	300	–	X	X	X	X
SP-9F	300	300	X	X	X	X
SP-10F	300	300	300	X	X	X
SP-11F	100	300	100	300	–	–
SP-12F	100	100	100	300	–	–
SP-13F	–	–	–	–	X	X
SP-14F	300	X	X	X	X	X
SP-15F	100	300	100	300	–	–
SP-16F	–	–	–	–	X	X
SP-17F	30	100	100	–	–	–
SP-18F	–	–	–	–	X	X
Phenytoin[a]	30	30	–	–	100	100
Ethosuximide [a]			100	300	–	–

The Number of animals used = 4; Solvent used- Polyethylene glycol; Dose of 30, 100 and 300 mg/kg were administered i.p. The figures in the table indicate the minimum dose where by bioactivity was demonstrated in half or more of the mice. The animals were examined at 0.5 h and 4 h after injections were administered.
The dash (–) indicates an absence of activity at maximum dose administered (300 mg/kg).
x-denotes compound was not tested.
[a] Data taken from Ref. [6] and dose in mg/kg.

scPTZ model only compound **SP-5F** showed protection at both time intervals at a dose level of 100 mg/kg, showing active nature of compound against absence seizure. Rest of the compounds was found to be active at a higher dose level of 300 mg/kg after 4 h time interval. Thus, optimal lipophilicity for anticonvulsant activity of pyridazinone analogues is around 2.03.

None of the tested compounds showed any sign of neurological deficit at the highest dose of 300 mg/kg.

Results of preliminary phase I anticonvulsant screening prompted us to further assess the most promising compound in phase II screening. The selected compound **SP-5F**was found to have significant anticonvulsant potential during Phase II study. As compared to standard drugs phenytoin and ethosuximide, compounds **SP-5F** demonstrated effective median dose (ED_{50}) 24.38 and 88.23 and higher protective index (PI) of 27.30 and 7.54 (Table 3) in MES and scPTZ screening respectively. The *p*-chlorophenyl substitution at pyridazinone was observed essential for better anticonvulsant activity.

To evaluate the GABA modulatory mechanism of pyridazinone analogue, whole brain GABA estimation of rats was carried out. Compound **SP-5F**, significantly increased the GABA level after both *i.p.* administration after 2 h and with an oral treatment for 7 days. After seven days of chronic oral administration, there was 1.74 folds increase in GABA level in rat brain as compared to control. Thus, the pyridazinone analogues might be acting through GABA modulatory mechanism (Table 4, Fig. 3).

Table 4
Effect of most potent compound in GABA system.

Compound	GABA level in mice brain (μg/100 mg of tissue) 2 h post treatment	7 days post treatment
SP-5F	72.4 ± 6.56*	90.1 ± 4.23*
Control	45.5 ± 5.03	51.5 ± 2.60
Clobazam	101 ± 6.77	110 ± 4.83

a) The compounds were tested at a dose of 100 mg/kg (i.p.) and clobazam (30 mg/ kg).
b) The data indicate the minimum concentration whereby at least 50% inhibition was demonstrated in one or more time points.
c) Each value represents the mean (SEM of six rats, significantly different from the control at.
* $p < 0.005$ (Student's *t*-test). Animal used – adult Wistar rats divided into three groups of six animals each.

It is well known that almost all AEDs like Carbamazepine and valporic acid are associated with hepatotoxicity [17]. Since most therapeutic agents limit the hepatotoxic reactions, the liver function test for all the compounds was performed. Result of the same has been shown in Table 5. The most active compound **SP-5F** was administered chronically to animals for 15 days and their biochemical parameters (SGOT, SGPT, alkaline phosphatase, total albumin and total protein) were evaluated. Compound **SP-5F** did not show any significant increase or decrease in the said parameters as shown in Table 4. By using hematoxylin and eosin staining technique, the histopathological evaluation of liver tissue of the groups which were treated with compound SP-5F showed histological features which were normal (Fig. 2) (see Table 6).

CNS bioavailability of a drug or molecule is greatly affected by various physicochemical descriptors such as LogP (partition coefficient), molecular weight (MW), hydrogen bond acceptors and donor counts. By using octanol-phosphate buffer method, the partition coefficient of all the compounds was determined experimentally (Table 1). The compounds were found to be lipophilic enough (> 2) with potential to cross the blood brain barrier which proves their anticonvulsant action potential. Due to high lipophilicity, rapid onset and shorter duration of action of the said compound may be reasoned. The log P values were found to be in optimal range of 1.38–3.56(< 5), otherwise it may lead to CNS toxicities like motor impairement etc. the topological polar surface area (TPSA) was calculated using Mol inspiration and the results have been presented in Table 5. The compounds showed %ABS from 80.24 to 83.42%. Number of rotatable bonds for the receptor binding is also crucial for conformational flexibilities. The number of rotatable bond should be < 10 for passing the oral bioavailability criteria. All the compounds in general possessed

Table 3
Phase II quantitative anticonvulsant evaluation in mice.

Comp.	ED_{50}[a] MES	scPTZ	TD_{50} [b]	PI[c] MES	scPTZ
SP-5F	24.38 (20.5–27.5)	88.23 (80.7–95.4)	665.7 (532.6–740.5)	27.30	7.54
Phenytoin [d]	9.5 (8.1–10.4)	> 300	65.5 (52.5–72.9)	6.9	< 0.22
Ethosuximide[d]	> 1000	130	440.8	< 0.44	3.39

Number of animals used = 10; Solvent used: polyethylene glycol (0.1 mL, i.p.).
[a] Median effective dose eliciting anticonvulsant protection in 50% animals.
[b] Median toxic dose eliciting minimal neurological toxicity in 50% animals.
[c] PI = Protective index (TD_{50}/ED_{50}).
[d] Data taken from Ref. [4] and dose in mg/kg.

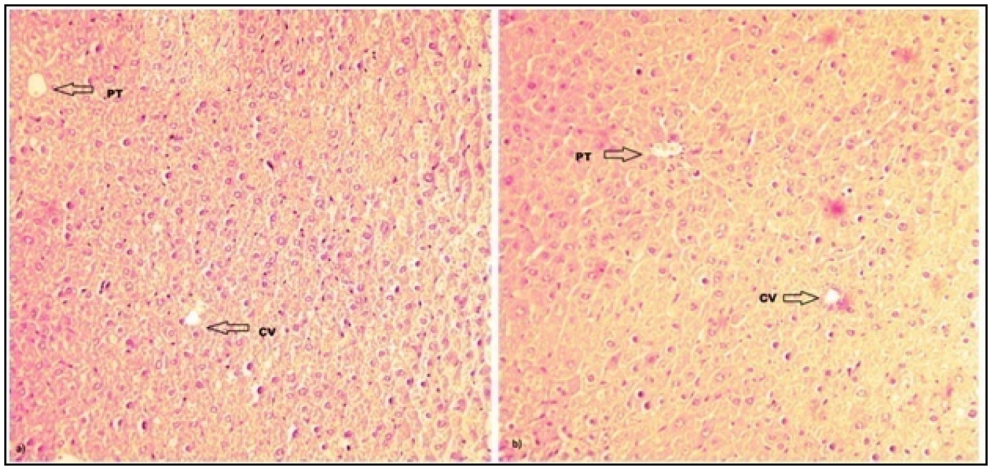

Fig. 2. High power photomicrograph of portal triad area of liver tissue from animals treated with (a) control (b) compound SP-5Fshowing a normal histological appearance (HE × 400). PT, portal triad; CV, central vein.

high number of rotatable bonds (3–5) and therefore provided fair conformational flexibility. No compounds violated Lipinski parameters (rule of 5), which makes them potential anticonvulsant agent.

2.3. Structure activity relationship

The results of anticonvulsant studies of the synthesized compounds (Table 1) indicated that electron withdrawing groups like (Cl, Br and F) on the phenyl attached at the 6th position of pyridazinone ring resulted into higher seizure protection. Electron donating group such as methyl, methoxy and dimethyl substituted phenyl did not show promising anticonvulsant activity. However, compounds with disubstituted methyl retains the anticonvulsant activity but at higher dose. Among the aliphatic chain substitution on phenyl ring, *n*-propyl was found to be more active than the isobutyl substitution. An introduction of groups which increase the length of molecules (biphenyl, phenoxyphenyl and benzyl phenyl), unsubstituted phenyl and heteroaromatic ring (thienyl) does not showed remarkable anticonvulsant activity except compound with napthyl ring. In general, following interesting pattern of anticonvulsant potencies of the phenyl ring substituents of the thiazole amide-pyridazinone derivatives were observed

p-chlorophenyl > *p*-bromophenyl > 3, 4-dichloro-phenyl > Naphthyl > p-fluorophenyl > *p*- Propyl phenyl > *p*-ethylbenzene > 3,4-Dimethylphenyl > *p*-Isobutyl phenyl > 2,4-Dimethylphenyl > *p*-tolyl > *p*-Anisyl > 2,5-Dimethylphenyl > Phenyl > *p*-Benzyl phenyl > thienyl > *p*-Biphenyl > *p*-Phenoxy phenyl.

2.4. Molecular docking studies

In this work, molecular docking computations were performed using Maestro 10.5 program (Schrodinger 2013, Inc., USA) to unleash the possible mechanism of anticonvulsant activity. The docking was performed on two main targets of commonly used anticonvulsant drugs: one is Na^+ channel and other is $GABA_A$ receptors. For this purpose, compound SP-5F was selected because it displayed most potent

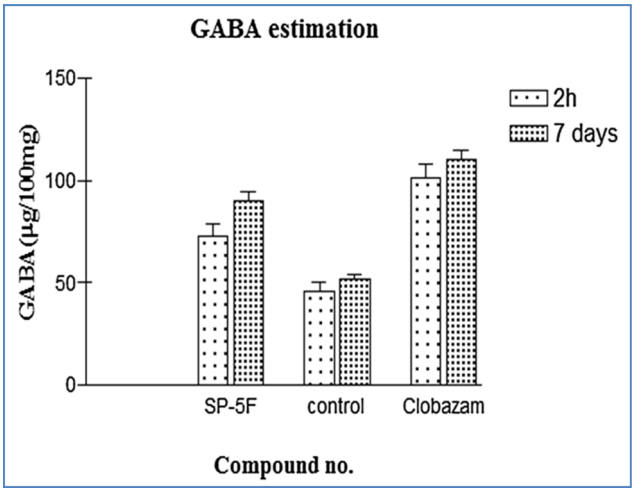

Fig. 3. Effect of compound **SP-5F** on GABA levels in mice brain tissues (µg/100 mg wet tissue).

anticonvulsant action against both (MES and scPTZ) animal screen models. Docking pose (Figs. 4 and 5) of compound SP-5F with a homology model of the Na^+ channel displayed that SP-5F bound to the receptor in a pocket formed of Asp7, Ala7C, Thr68D, Ser69D, Phe80, Phe84, Val87, Leu88, Phe91, Ser83, Thr87, Phe84 and Lys7D. Among these amino acid residues, SP-5F formed two hydrogen bonds, one hydrogen bond formed between the amino group of thiazole with Asp7 and the other between the keto groups of pyridazinone with Lys7D. The docking and gliding scores were found to be −5.291 and −4.160 within docking interaction of SP-5F with a homology model of the voltage-gated sodium channel receptor. The docking study of compound SP-5F with $GABA_A$ receptor was also carried out and docking pose (Figs. 6 and 7) showed that SP-5F was surrounded by $GABA_A$ receptors. Binding interaction of SP-5F with $GABA_A$ showed that it was

Table 5
Liver enzyme and total protein estimation of the most potent compound SP-5F.

Comp.[a]	SGOT ± SEM	SGPT ± SEM	Alkaline phosphatase ± SEM	Total albumin(g/100 mL) ± SEM	Total protein (g/100 mL) ± SEM
SP-5F	40.12 ± 1.90	37.58 ± 1.85	58.13 ± 2.08	1.63 ± 0.024	5.28 ± 0.24*
control[b]	37.18 ± 1.71	34.23 ± 1.27	56.11 ± 2.01	1.56 ± 0.021	5.23 ± 0.21

[a] Relative to control and data were analyzed by ANOVA followed by Student's *t* test for n = 4 at.
* $p < 0.05$.
[b] Control group were treated with 0.5% methyl cellulose for 15 days.

Table 6
Important pharmacokinetics parameters for good oral bioavailability of title compounds (SP-1F to SP-18F).

Comp.	R	% ABS	TPSA (A^2)	*n*-rotb	Mol.Wt.	Molar Vol.	mi LogP	*n*-OHNH donor	n- ON acceptor	Lipinski's violation
Rule					< 500		< 5	< 5	< 10	< 1
SP-1F	Phenyl	83.42	74.14	4	316.39	274.17	1.48	1	6	0
SP-2F	*p*-Fluro-phenyl	83.42	74.14	4	334.38	279.10	1.64	1	6	0
SP-3F	*p*-Tolyl	83.42	74.14	4	330.41	290.73	1.93	1	6	0
SP-4F	*p*-Anisyl	80.24	83.37	5	346.41	299.72	1.53	1	7	0
SP-5F	*p*-Chloro-phenyl	83.42	74.14	4	350.83	287.71	2.15	1	6	0
SP-6F	*p*-Ethylphenyl	83.42	74.14	5	344.44	307.53	2.39	1	6	0
SP-7F	3,4-Dimethylphenyl	83.42	74.14	4	344.44	307.29	2.30	1	6	0
SP-8F	2,5-Dimethylphenyl	83.42	74.14	4	344.44	307.29	2.30	1	6	0
SP-9F	2,4-Dimethylphenyl	83.42	74.14	4	344.44	307.29	2.30	1	6	0
SP-10F	*p*- Isobutyl phenyl	83.42	74.14	7	386.52	357.73	3.56	1	6	0
SP-11F	β- Nephthyl	83.42	74.14	4	366.45	318.16	2.64	1	6	0
SP-12F	3,4-Dichloro-phenyl	83.42	74.14	4	385.28	301.24	2.76	1	6	0
SP-13F	*p*- Benzyl phenyl	83.42	74.14	6	406.51	362.38	3.44	1	6	0
SP-14F	*p*- Phenoxy phenyl	80.24	83.37	6	408.48	354.56	3.23	1	7	0
SP-15F	*p*-Propyl phenyl	83.42	74.14	6	358.47	324.34	2.78	1	6	0
SP-16F	*p*-Biphenyl	83.42	74.14	5	392.48	345.58	3.27	1	6	0
SP-17F	*p*-Bromo-phenyl	83.42	74.14	4	395.28	292.06	2.29	1	6	0
SP-18F	2-Thienyl	83.42	74.14	4	322.42	264.88	1.38	1	6	0

% ABS percentage of absorption, TPSA topological polar surface area, *n*-ROTB number of rotatable bonds, MW molecular weight, MV molecular volume, *n*-OHNH number of hydrogen bond donors, *n*-ON number of hydrogen bond acceptors.

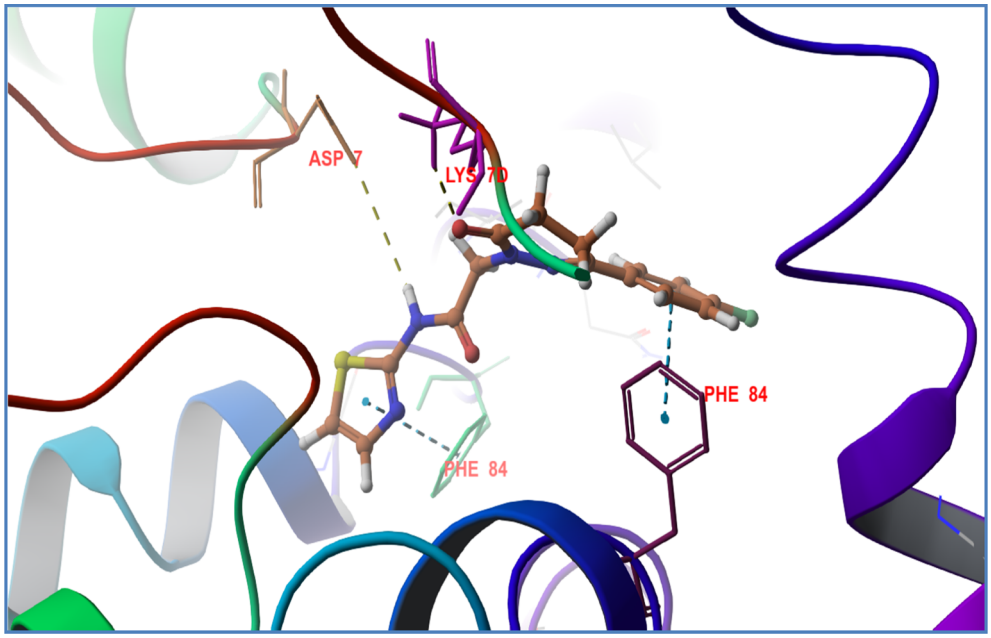

Fig. 4. Binding mode of compound SP-5F into voltage-gated sodium channel receptor pocket (homology model). Hydrogen bonds are shown with yellow dotted lines. One hydrogen bond is between NH of thiazole and aspartate7 shown in brown color and other is between keto groups of pyridazinone and lysine 7D shown in purple color.

bound to a site formed of Val202, His101, Tyr159, Tyr209, Val211, Arg132, Lue131, Phe77, Met130, Leu140, Thr142, Ser204, Glu189, Thr206, Thr141, Phe99, Gly157, Ser158, Val210 and Ser204. Hydrogen bonds are shown with yellow dotted lines and pi-pi interaction by blue dotted lines. The compounds (SP-5F) showed four hydrogen bonds; among them two of the hydrogen bond is with common amino acid Thr 206 and the C=O group of the pyridazinone and the aliphatic amide chain. The NH of the amide group showed key interaction with Tyr 159. This underscores the importance of C=O and NH group present in the compound.

The docking and gliding scores of compound (SP-5F) with $GABA_A$ docking interaction were found to be −7.357 and −6.714. Lastly, the result of docking interaction of the compound SP-5F showed that it forms four hydrogen bonds with the $GABA_A$ receptor with a high docking score as well as high gliding score, whereas the binding interaction with Na^+ channel receptor gave less hydrogen bonding, less docking as well as less gliding score. Hence, it may be concluded that our compounds better act by $GABA_A$ receptors rather than Na^+ channel blocker.

2.5. Pharmacophore distance mapping

The distance between various groups [one aryl (R) hydrophobic domain, one electron donor (D), and a hydrogen bond acceptor/donor unit (HBD)] essential for anticonvulsant activity were calculated using 3D optimized structures using ACD freeware 3D viewer 12.0 version. Fig. 8 shows the distances between various groups of standard drugs postulated essential for the anticonvulsant. The results of pharmacophore distance mapping of six standard antiepileptic drugs were then compared with most active compound **(SP-5F)** are shown in Table 7. It was found that the distance between various groups essential for anticonvulsant action was in good agreement with the clinically available AEDs.

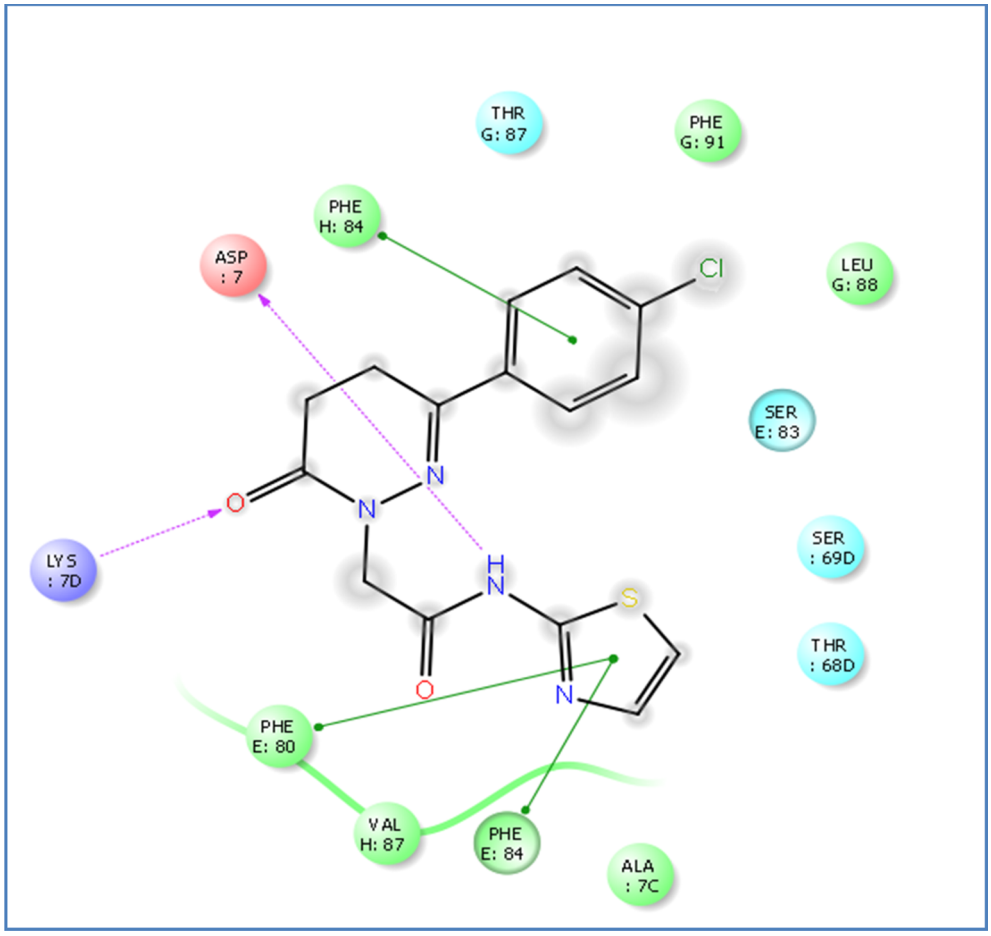

Fig. 5. Lig plot of compound SP-5F showing interaction into the binding site of Na^+ channel receptor (homology model).

3. Conclusion

In continuation of our previous studies on pyridazinone analogues as anticonvulsant, a series of hybrid thiazole-pyridazinone analogues were synthesized as anticonvulsants. Among all eighteen synthesized compounds, 2-(3-(4-chlorophenyl)-6-oxo-5,6-dihydropyridazin-1(4H)-yl)-N-(thiazol-2-yl)acetamide (**SP-5F**) emerged as the most potent and safer anticonvulsant agent acting through GABA mediated mechanism.

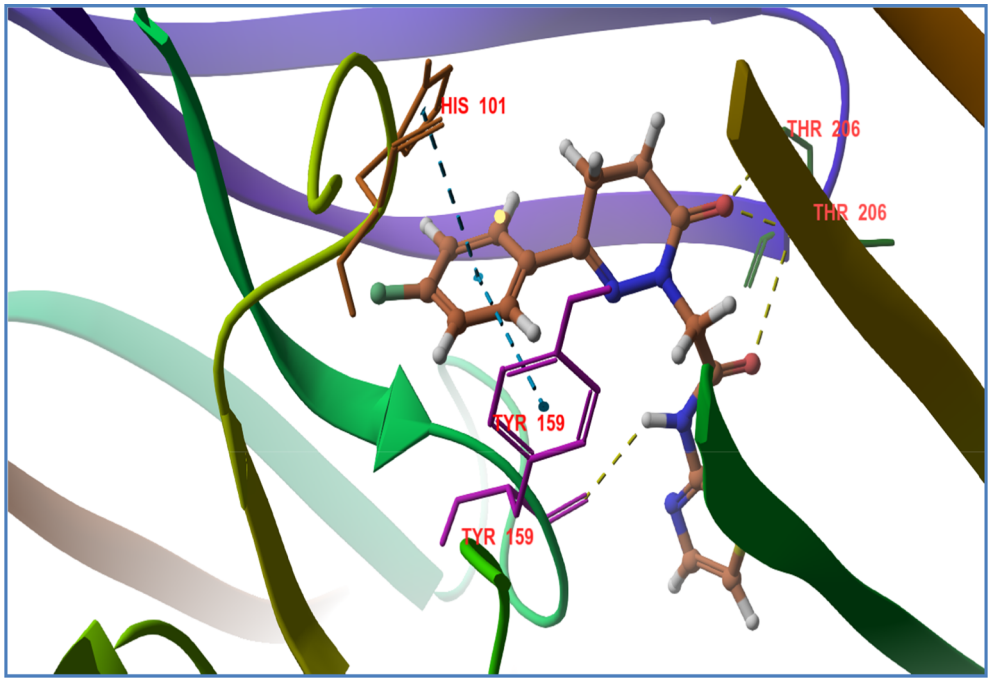

Fig. 6. Binding mode of compound SP-5F into the $GABA_A$ receptor pocket (homology model). Hydrogen bonds are shown with yellow dotted lines and pi-pi interaction by blue dotted lines. The compounds showed four hydrogen bonds; among them two of the hydrogen bond is with common amino acid Thr 206 and the C═O group of the pyridazinoneand the aliphaticamide chain. The NH of the amide group showed key interaction with Tyr 159. This underscores the importance of C═O and NH group present in the compound.

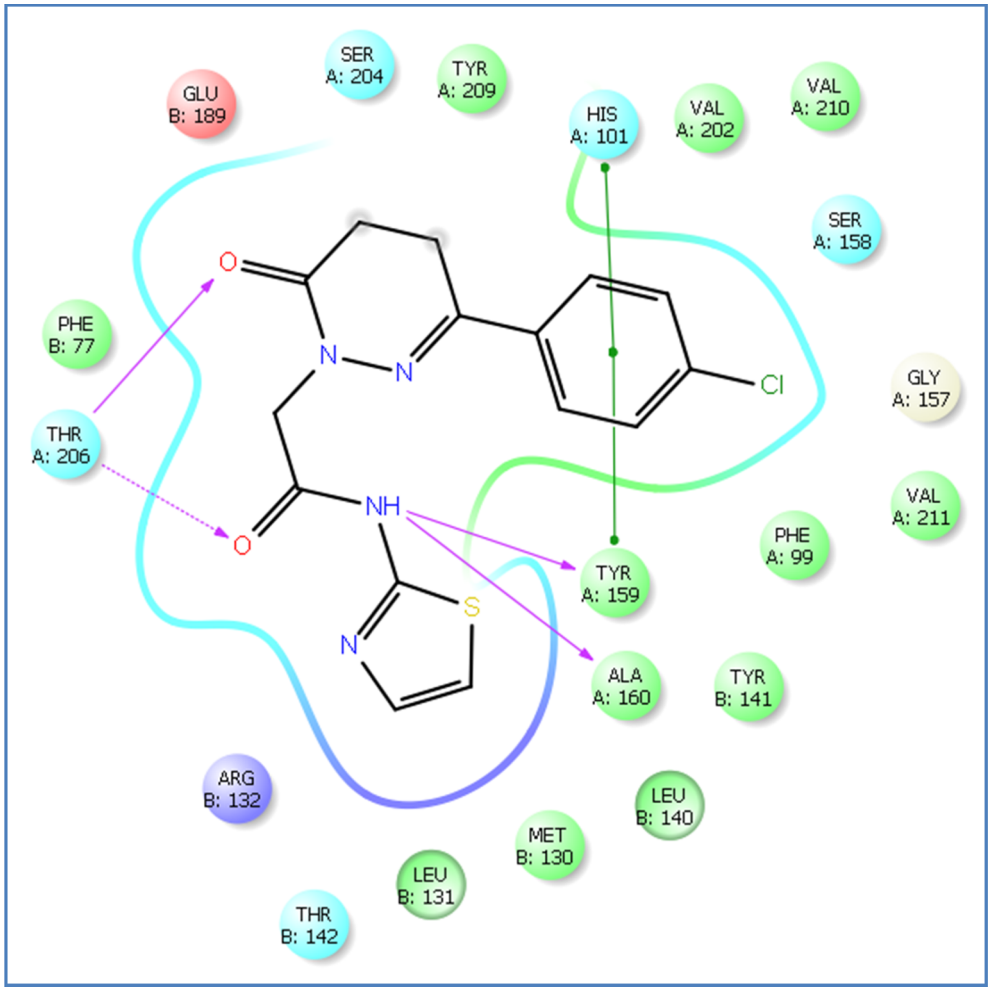

Fig. 7. Lig plot of compound SP-5F showing interaction into the $GABA_A$ receptor pocket (homology model).

In silico pharmacophoric pattern and drug likeness studies showed that all the compounds fulfill the requirements which are crucial to be a potent anticonvulsant drug. Further, molecular docking studies on the validated target protein substantiate the binding pattern of the ligand as hypothesized by the pharmacophore pattern. Thus, hybrid thiazole-pyridazinones may lead to the development of ideal scaffolds for anticonvulsant agents acting through GABA mediated mechanism.

4. Experimental

4.1. General

All the chemicals used were of laboratory grade and procured from E. Merck (Darmstadt, Germany) and S.D. Fine Chemicals (Mumbai, India). Melting points were determined by open capillary tubes in a Hicon melting point apparatus (Hicon, New Delhi, India) and are uncorrected. Purity of the compounds was checked by thin-layer chromatography (TLC) plates (silica gel G) by using ethylacetate: Hexane

Table 7
Distance range between the essential structural elements R, D and HBD.

Compound	R-HBD[a]	R-D[a]	D-HBD[a]
Gabapentin	4.02	4.14	4.45
Phenytoin	4.97	5.22	4.63
Carbamazepine	6.51	4.61	3.44
Remacemide	5.06	6.74	4.37
Progabide	6.65	4.49	5.12
SP-5F	6.38	6.03	3.95

[a] Distances calculated for 3D optimized structures using MM3 and CHARMM parameterization (Argus Lab 4.0 and ACD/3D viewer).

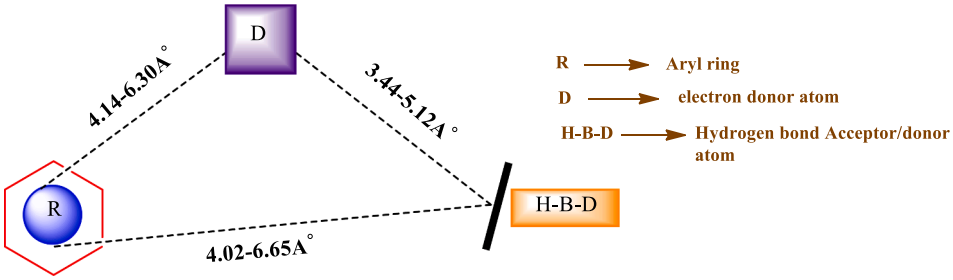

Fig. 8. Distance range between the essential structural elements R, D and HBD.

(4:6), which were visualized by exposing to iodine vapours and UV light. The FT-IR spectra were recorded on (IR affinity SHIMADZU) FTIR spectrophotometer using KBrpellets; υ_{max} values are given in cm^{-1} and ^1H NMR spectra were recorded on Bruker model DRX-300 and 400 MHz NMR spectrometer (^1H at 300 and 400 MHz, ^{13}C at 100 MHz) in DMSO-d_6. Chemical shifts (δ) are expressed in ppm relative to tetramethylsilane (TMS) as an internal standard and coupling constants (J values) are expressed in Hz. Mass spectra were recorded on LCMS/MS (Perkin Elmer and LABINDIA, Applied Biosystem) model no. API 3000, presented as m/z. Elemental analysis (C, H and N) were undertaken with Perkin-Elmer model 240C analyzer. Analyses for C, H, and N were within ± 0.4% of the theoretical values.

4.2. General procedure for the synthesis of 6-substituted-phenyl- 4, 5-dihydropyridazin-3(2H)-one (SP-1b to SP-18b)

The appropriate substituted β-aroyl propionic acids were reacted with hydrazine hydrate to get corresponding pyridazinone and characterized on the basis of spectral data as per earlier reported procedure [16].

4.2.1. General procedure for the synthesis of 2-(6-oxo-3-substitutedaryl-5,6-dihydropyridazin-1(4H)-yl)-N-(thiazol-2-yl)acetamide(SP-1F to SP-18F)

To a mixture of 6-substituted-phenyl- 4, 5-dihydropyridazin-3(2*H*)-one (0.01 mol) (SP-2b to SP-18b) and 2-chloro-N-(thiazol-2-yl) acetamide (0.02 mol) in dry DMF (10 mL) was added potassium carbonate. The reaction mixture was reflux for 5 h until TLC showed the single spot. It was cooled and poured into crushed ice. The solid obtained was filtered and recrystallized with methanol.

4.2.2. 2-(6-oxo-3phenyl-5, 6-dihydropyridazin-1(4H)-yl)-N-(thiazol-2-yl) acetamide (SP-1F)

Yield: 46%; mp 189–191 °C; R_f = 0.48; IR (KBr) (cm^{-1}): 3350 (N—H str), 1695 (C═O str), 1562 (C═N str); ^1H NMR (400 MHz, DMSO-d_6) δ(ppm): 9.37 (s, 1H, NH), 7.82–7.67(m, 5H, phenyl), 7.53 (d, J = 7.8, H4-thiazole), 7.29 (d, J = 4.3, H3-thiazole), 3.89 (s, 2H, —CH_2), 2.98 (t, J = 7.8, 2H, C—CH_2), 2.53 (t, J = 7.8, 2H, CH_2-CO Pyridazinone). ^{13}C NMR (100 MHz, DMSO-d_6) δ (ppm): 168.40, 162.12, 159.50, 145.87, 136.25, 132.73, 130.94, 128.30, 126.59, 112.37, 54.80, 32.48 and 24.64. Mass (m/z): 315[M + 1]; Anal. Calcd. for $C_{15}H_{14}N_4O_2S$: C, 57.31; H, 4.49; N, 17.82; Found: C, 57.34; H, 4.51; N, 17.85.

4.2.3. 2-(3-(4-fluorophenyl)-6-oxo-5,6-dihydropyridazin-1(4H)-yl)-N-(thiazol-2-yl)acetamide (SP-2F)

Yield: 57%; mp 238–242 °C; R_f = 0.64; IR (KBr) (cm^{-1}): 3431 (N—H str), 1705 (C═O str), 1615 (C═N str); ^1H NMR (400 MHz, DMSO-d_6) δ(ppm): 9.36 (s, 1H, NH), 7.98–7.64 (m, 4H, phenyl), 7.52 (d, J = 7.6, H4-thiazole), 7.38 (d, J = 4.2, H3-thiazole), 3.87 (s, 2H, —CH_2), 2.96 (t, J = 7.8, 2H, C—CH_2), 2.54 (t, J = 7.8, 2H, CH_2-CO Pyridazinone). ^{13}C NMR (100 MHz, DMSO-d_6) δ (ppm): 168.21, 162.10, 165.32, 159.76, 146.23, 132.49, 131.92, 129.32, 115.85, 112.78, 54.67, 32.56 and 24.79. ESI MS (m/z): 333 [M + 1]; Anal. Calcd. for $C_{15}H_{13}FN_4O_2S$: C, 54.21; H, 3.94; N, 16.86; Found: C, 54.24; H, 3.97; N, 16.89;

4.2.4. 2-(6-oxo-3-(p-tolyl)-5,6-dihydropyridazin-1(4H)-yl)-N-(thiazol-2-yl)acetamide (SP-3F)

Yield: 76%; mp 270–272 °C; R_f = 0.73; IR (KBr) (cm^{-1}): 3346 (N—H str), 1690 (C═O str), 1612 (C═N str); ^1H NMR (400 MHz, DMSO-d_6) δ(ppm): 9.33 (s, 1H, NH), 8.59–8.35 (m, 4H, phenyl), 7.54 (d, J = 8.8, H4-thiazole), 7.04 (d, J = 4.8, H3-thiazole), 4.67 (s, 2H, —CH_2), 2.80 (t, J = 8.0, 2H, C—CH_2), 2.45 (t, J = 8.0, 2H, CH_2-CO Pyridazinone), 2.32 (s, 3H, CH_3). ^{13}C NMR (100 MHz, DMSO-d_6) δ (ppm): 167.96, 162.71, 162.42, 146.59, 140.86, 133.20, 132.09, 129.62, 127.56, 112.76, 54.82, 32.66, 24.10, and 21.89. ESI MS (m/z): 329[M + 1]; Anal. Calcd. for $C_{16}H_{16}N_4O_2S$: C, 58.52; H, 3.94; N, 16.86; Found: C, 58.54; H, 3.97; N, 16.89.

4.2.5. 2-(3-(4-methoxyphenyl)-6-oxo-5,6-dihydropyridazin-1(4H)-yl)-N-(thiazol-2-yl)acetamide(SP-4F)

Yield: 38%; mp 218–220 °C; R_f = 0.55; IR (KBr) (cm^{-1}): 3446 (N—H str), 1697 (C═O str), 1644 (C═N str); ^1H NMR (400 MHz, DMSO-d_6) δ(ppm): 9.47 (s, 1H, NH), 7.92–7.72 (m, 4H, phenyl), 7.53 (d, J = 7.4, H4-thiazole), 7.29 (d, J = 4.1, H3-thiazole), 3.84 (s, 3H, —OCH_3), 3.56 (s, 2H, —CH_2), 2.92 (t, J = 7.8, 2H, C—CH_2), 2.54 (t, J = 7.8, 2H, CH_2-CO Pyridazinone). ^{13}C NMR (100 MHz, DMSO-d_6) δ (ppm): 168.37, 162.96, 162.54, 162.01, 146.27, 132.81, 128.76, 114.98, 112.08, 55.81, 54.28, 32.87 and 24.65. ESI MS (m/z): 345[M + 1]; Anal. Calcd. for $C_{16}H_{16}N_4O_3S$: C, 55.80; H, 4.68; N, 16.27; Found: C, 55.82; H, 4.70; N, 16.29.

4.2.6. 2-(3-(4-chlorophenyl)-6-oxo-5,6-dihydropyridazin-1(4H)-yl)-N-(thiazol-2-yl)acetamide(SP-5F)

Yield: 68%; mp 262–264 °C; R_f = 0.61; IR (KBr) (cm^{-1}): 3410 (N—H str), 1640 (C═O str), 1617 (C═N str); ^1H NMR (400 MHz, DMSO-d_6) δ(ppm): 9.32 (s, 1H, NH), 7.80–8.12 (m, 4H, phenyl), 7.41 (d, J = 7.8, H4-thiazole), 7.15 (d, J = 4.5, H3-thiazole), 3.92 (s, 2H, —CH_2), 3.62 (t, J = 7.8, 2H, C—CH_2), 2.42 (t, J = 7.8, 2H, CH_2-CO Pyridazinone). ^{13}C NMR (100 MHz, DMSO-d_6) δ (ppm): 168.29, 165.16, 162.90, 162.44, 146.36, 136.67, 132.46, 128.83, 128.64, 112.28, 56.25, 54.12, 32.12 and 24.28. ESI MS (m/z): [M + 1], 350[M + 2]; Anal. Calcd. for $C_{15}H_{13}ClN_4O_2S$: C, 51.65; H, 3.76; N, 16.06; Found: C, 51.68; H, 3.77; N, 16.08.

4.2.7. 2-(3-(4-ethylphenyl)-6-oxo-5,6-dihydropyridazin-1(4H)-yl)-N-(thiazol-2-yl)acetamide(SP-6F)

Yield: 60%; mp 298–300 °C; R_f = 0.42; IR (KBr) (cm^{-1}): 3360 (N—H str), 1685 (C═O str), 1635 (C═N str); ^1H NMR (400 MHz, DMSO-d_6) δ(ppm): 9.46 (s, 1H, NH), 7.72–8.06 (m, 4H, phenyl), 7.41 (d, J = 7.6, H4-thiazole), 7.23 (d, J = 4.6, H3-thiazole), 3.87 (s, 2H, —CH_2), 2.96 (t, J = 7.8, 2H, C—CH_2), 2.52 (q, 2H, —CH_2CH_3), 2.52 (t, J = 7.8, 2H, CH_2-CO Pyridazinone), 1.23 (t, 3H, —CH_3). ^{13}C NMR (100 MHz, DMSO-d_6) δ (ppm): 167.98, 165.46, 162.79, 147.08, 146.35, 133.48, 132.24, 127.99, 127.24, 112.46, 54.78, 32.42, 30.15, 24.12 and 16.52. ESI MS (m/z): 343[M + 1]; Anal. Calcd. for $C_{17}H_{18}N_4O_2S$: C, 59.63; H, 5.30; N, 16.36; Found: C, 59.66; H, 5.32; N, 16.38.

4.2.8. 2-(3-(3,4-dimethylphenyl)-6-oxo-5,6-dihydropyridazin-1(4H)-yl)-N-(thiazol-2-yl)acetamide(SP-7F)

Yield: 44%; mp 258–260 °C; R_f = 0.68; IR (KBr) (cm^{-1}): 3450 (N—H str), 1710 (C═O str), 1599 (C═N str); ^1H NMR (400 MHz, DMSO-d_6) δ(ppm): 9.26 (s, 1H, NH), 7.54–7.78 (m, 3H, phenyl), 7.45 (d, J = 7.8, H4-thiazole), 7.30 (d, J = 4.4, H3-thiazole), 3.58 (s, 2H, —CH_2), 2.96 (t, J = 7.8, 2H, C—CH_2), 2.46 (t, J = 7.8, 2H, CH_2-CO Pyridazinone), 2.32 (s, 6H, CH_3). ^{13}C NMR (100 MHz, DMSO-d_6) δ (ppm): 168.44, 162.88, 162.08, 146.50, 139.76, 136.57, 132.61, 132.29, 130.82, 129.15, 124.82, 112.25, 54.79, 34.23, 32.46, 25.03. ESI MS (m/z): 343[M + 1]; Anal. Calcd. for $C_{17}H_{18}N_4O_2S$: C, 59.63; H, 5.30; N, 17.82; Found: C, 57.35; H, 4.52; N, 17.85.

4.2.9. 2-(3-(2,5-dimethylphenyl)-6-oxo-5,6-dihydropyridazin-1(4H)-yl)-N-(thiazol-2-yl)acetamide(SP-8F)

Yield: 59%; mp 248–250 °C; R_f = 0.51; IR (KBr) (cm^{-1}): 3360 (N—H str), 1690 (C═O str), 1609 (C═N str); ^1H NMR (400 MHz, DMSO-d_6) δ(ppm): 9.41 (s, 1H, NH), 7.71–7.54 (m, 3H, phenyl), 7.41 (d, J = 7.6, H4-thiazole), 7.33 (d, J = 4.6, H3-thiazole), 3.74 (s, 2H, —CH_2), 2.94 (t, J = 7.8, 2H, C—CH_2), 2.53 (t, J = 7.8, 2H, CH_2-CO Pyridazinone), 2.46 (m, 6H, CH_3). ^{13}C NMR (100 MHz, DMSO-d_6) δ (ppm): 168.51, 162.98, 162.17, 146.94, 135.63, 132.97, 132.01, 131.19, 130.37, 129.52, 128.80, 112.75, 54.62, 32.19, 24.67, 21.20, and 19.53. ESI MS (m/z): 343[M + 1]; Anal. Calcd. for $C_{17}H_{18}N_4O_2S$: C, 59.63; H, 5.30; N, 17.82; Found: C, 57.35; H, 4.52; N, 17.85.

4.2.10. 2-(3-(2,4-dimethylphenyl)-6-oxo-5,6-dihydropyridazin-1(4H)-yl)-N-(thiazol-2-yl)acetamide(SP-9F)

Yield: 58%; mp 254–256 °C; R_f = 0.48; IR (KBr) (cm^{-1}): 3420 (N—H str), 1710 (C═O str), 1660 (C═N str); ^{1}H NMR (400 MHz, DMSO-d_6) δ(ppm): 9.51 (s, 1H, NH), 7.70–7.59 (m, 3H, phenyl), 7.48 (d, J = 7.2, H4-thiazole), 7.28 (d, J = 4.1, H3-thiazole), 3.92 (s, 2H, $-CH_2$), 2.96 (t, J = 7.8 Hz, 2H, C$-CH_2$), 2.43 (t, J = 7.8, 2H, CH_2-CO Pyridazinone), 2.51 (m, 6H, CH_3). ^{13}C NMR (100 MHz, DMSO-d_6) δ (ppm): 167.93, 162.87, 162.04, 146.34, 138.61, 136.90, 131.09, 132.45, 129.18, 126.88, 126.03, 112.44, 54.63, 32.57, 31.26, 25.72 and 24.38. ESI MS (m/z): 343[M + 1]; Anal. Calcd. for $C_{17}H_{18}N_4O_2S$: C, 59.63; H, 5.30; N, 17.82; Found: C, 57.35; H, 4.52; N, 17.85.

4.2.11. 2-(3-(4-isobutylphenyl)-6-oxo-5,6-dihydropyridazin-1(4H)-yl)-N-(thiazol-2-yl)acetamide(SP-10F)

Yield: 47%; mp 290–292 °C; R_f = 0.72; IR (KBr) (cm^{-1}): 3345 (N—H str), 1725 (C═O str), 1592 (C═N str); ^{1}H NMR (400 MHz, DMSO-d_6) δ(ppm): 9.43 (s, 1H, NH), 7.54–7.78 (m, 4H, phenyl), 7.41 (d, J = 7.4, H4-thiazole), 7.25 (d, J = 4.8, H3-thiazole), 3.84 (s, 2H, $-CH_2$), 2.98 (t, J = 7.8, 2H, C$-CH_2$), 2.43 (t, J = 7.8, 2H, CH_2-CO Pyridazinone), 0.91 (d, 6H, $(CH_3)_2$, 1.63–1.71 (m, 1H, −CH), 1.98 (d, 2H, $-CH_2$). ^{13}C NMR (100 MHz, DMSO-d_6) δ (ppm): 168.76, 162.80, 162.01, 146.38, 143.76, 133.59, 132.06, 128.46, 126.65, 112.50, 54.78, 44.61, 32.19, 29.48, 24.15 and 22.71. ESI MS (m/z): 371[M + 1]; Anal. Calcd. for $C_{19}H_{22}N_4O_2S$: C, 61.60; H, 5.99; N, 15.12; Found: C, 61.62; H, 6.01; N, 15.15.

4.2.12. 2-(3-(naphthalen-1-yl)-6-oxo-5,6-dihydropyridazin-1(4H)-yl)-N-(thiazol-2-yl)acetamide (SP-11F)

Yield: 63%; mp 268–270 °C; R_f = 0.57; IR (KBr) (cm^{-1}): 3355 (N—H str), 1700 (C═O str), 1602 (C═N str); ^{1}H NMR (400 MHz, DMSO-d_6) δ(ppm): 9.27 (s, 1H, NH), 7.96–7.75 (m, 7H, phenyl), 7.54 (d, J = 7.6, H4-thiazole), 7.35 (d, J = 4.6, H3-thiazole), 3.86 (s, 2H, $-CH_2$), 2.96 (t, J = 7.8, 2H, C$-CH_2$), 2.43 (t, J = 7.8, 2H, CH_2-CO Pyridazinone). ^{13}C NMR (100 MHz, DMSO-d_6) δ (ppm): 168.45, 162.97, 162.10, 146.67, 134.52, 133.18, 132.85, 130.27, 129.04, 127.25, 126.12, 125.39, 112.24, 54.68, 32.81 and 24.86. ESI MS (m/z): 365[M + 1]; Anal. Calcd. for $C_{19}H_{16}N_4O_2S$: C, 62.62; H, 4.49; N, 17.82; Found: C, 62.66; H, 4.51; N, 17.86.

4.2.13. 2-(3-(3,4-dichlorophenyl)-6-oxo-5,6-dihydropyridazin-1(4H)-yl)-N-(thiazol-2-yl)acetamide (SP-12F)

Yield: 70%; mp 178–180 °C; R_f = 0.62; IR (KBr) (cm^{-1}): 3360 (N—H str), 1685 (C═O str), 1610 (C═N str); ^{1}H NMR (400 MHz, DMSO-d_6) δ(ppm): 9.48 (s, 1H, NH), 7.67–7.86 (m, 3H, phenyl), 7.50 (d, J = 7.8, H4-thiazole), 7.34 (d, J = 4.2, H3-thiazole), 3.87 (s, 2H, $-CH_2$), 2.94 (t, J = 7.8, 2H, C$-CH_2$), 2.48 (t, J = 7.8, 2H, CH_2-CO Pyridazinone). ^{13}C NMR (100 MHz, DMSO-d_6) δ (ppm): 168.44, 162.95, 162.14, 146.58, 135.77, 133.95, 132.96, 130.49, 129.22, 126.82, 112.44, 54.92, 32.61 and 24.74. ESI MS (m/z): 383[M + 1], 384[M + 2]; Anal. Calcd. for $C_{15}H_{12}Cl_2N_4O_2S$: C, 47.01; H, 3.16; N, 14.62; Found: C, 47.04; H, 3.18; N, 14.65.

4.2.14. 2-(3-(4-benzylphenyl)-6-oxo-5,6-dihydropyridazin-1(4H)-yl)-N-(thiazol-2-yl)acetamide (SP-13F)

Yield: 40%; mp 201–203 °C; R_f = 0.48; IR (KBr) (cm^{-1}): 3450 (N—H str), 1699 (C═O str), 1600 (C═N str); ^{1}H NMR (400 MHz, DMSO-d_6) δ(ppm): 9.51 (s, 1H, NH), 7.99–7.74 (m, 9H, phenyl), 7.46 (d, J = 7.1, H4-thiazole), 7.39 (d, J = 7.6, H3-thiazole), 3.86 (s, 2H, $-CH_2$), 3.42 (s, 2H, $-CH_2$), 2.98 (t, J = 7.8, 2H, C$-CH_2$), 2.53 (t, J = 7.8, 2H, CH_2-CO Pyridazinone). ^{13}C NMR (100 MHz, DMSO-d_6) δ (ppm): 168.74, 162.79, 162.02, 146.65, 143.85, 141.25, 136.13, 133.78, 132.56, 129.44, 128.62, 127.17, 126.02, 112.42, 54.28, 41.34, 32.14 and 24.64. ESI MS (m/z): 405[M + 1]; Anal. Calcd. for $C_{22}H_{20}N_4O_2S$: C, 65.33; H, 4.98; N, 13.85; Found: C, 65.35; H, 4.99; N, 13.87.

4.2.15. 2-(6-oxo 3-(4-phenoxyphenyl)-5,6-dihydropyridazin-1(4H)-yl)-N-(thiazol-2-yl)acetamide (SP-14F)

Yield: 56%; mp 229–231 °C; R_f = 0.71; IR (KBr) (cm^{-1}): 3487 (N—H str), 1720 (C═O str), 1585 (C═N str); ^{1}H NMR (400 MHz, DMSO-d_6) δ(ppm): 9.34 (s, 1H, NH), 7.89–7.64 (m, 9H, phenyl), 7.52 (d, J = 7.2, H4-thiazole), 7.27 (d, J = 4.6, H3-thiazole), 3.76 (s, 2H, $-CH_2$), 2.91 (t, J = 7.8, 2H, C$-CH_2$), 2.44 (t, J = 7.8, 2H, CH_2-CO Pyridazinone). ^{13}C NMR (100 MHz, DMSO-d_6) δ (ppm): 168.21, 162.91, 159.58, 157.43, 145.38, 136.12, 132.47, 130.59, 128.33, 126.59, 121.11, 118.23, 117.52, 112.53, 54.03, 32.84 and 24.83. ESI MS (m/z): 407[M + 1]; Anal. Calcd. for $C_{21}H_{18}N_4O_3S$: C, 62.05; H, 4.46; N, 13.78; Found: C, 62.07; H, 4.48; N, 13.79.

4.2.16. 2-(6-oxo 3-(4-propylphenyl)-5,6-dihydropyridazin-1(4H)-yl)-N-(thiazol-2-yl)acetamide (SP-15F)

Yield: 38%; mp 287–289 °C; R_f = 0.58; IR (KBr) (cm^{-1}): 3325 (N—H str), 1640 (C═O str), 1620 (C═N str); ^{1}H NMR (400 MHz, DMSO-d_6) δ(ppm): 9.29 (s, 1H, NH), 7.81–7.58 (m, 4H, phenyl), 7.43 (d, J = 7.2, H4-thiazole), 7.31 (d, J = 4.6, H3-thiazole), 3.76 (s, 2H, $-CH_2$), 2.90 (t, J = 7.8, 2H, C$-CH_2$), 2.60 (t, J = 3.6, 2H, $-CH_2CH_2$), 2.47 (t, J = 7.8, 2H, CH_2-CO Pyridazinone), 1.62 (m, 2H, $-CH_2CH_3$), 1.10 (t, J = 3.2, 3H, $-CH_2CH_3$) . ^{13}C NMR (100 MHz, DMSO-d_6) δ (ppm): 167.96, 162.71, 159.55, 145.78, 136.12, 132.57, 130.89, 128.63, 126.59, 112.43, 54.18, 37.40, 32.04, 24.64, 24.10, and 15.76. ESI MS (m/z): 357[M + 1]; Anal. Calcd. for $C_{18}H_{20}N_4O_2S$: C, 60.65; H, 5.66; N, 15.72; Found: C, 60.68; H, 5.69; N, 15.74.

4.2.17. 2-(3-([1,1′-biphenyl]-4-yl)-6-oxo-5,6-dihydropyridazin-1(4H)-yl)-N-(thiazol-2-yl)acetamide(SP-16F)

Yield: 32%; mp 244–246 °C; R_f = 0.76; IR (KBr) (cm^{-1}): 3368 (N—H str), 1699 (C═O str), 1578 (C═N str); ^{1}H NMR (400 MHz, DMSO-d_6) δ(ppm): 9.33 (s, 1H, NH), 7.96–7.54 (m, 9H, phenyl), 7.45 (d, J = 7.8, H4-thiazole), 7.33 (d, J = 4.4, H3-thiazole), 3.80 (s, 2H, $-CH_2$), 2.96 (t, J = 7.8, 2H, C$-CH_2$), 2.48 (t, J = 7.8, 2H, CH_2-CO Pyridazinone). ^{13}C NMR (100 MHz, DMSO-d_6) δ (ppm): 168.04, 162.74, 159.63, 145.48, 143.59, 140.75, 136.52, 132.97, 130.09, 129.51, 128.73, 1127.49, 126.49, 112.33, 54.13, 32.74 and 24.53. ESI MS (m/z): 391[M + 1]; Anal. Calcd. for $C_{21}H_{18}N_4O_2S$: C, 64.60; H, 4.65; N, 14.35; Found: C, 64.62; H, 4.67; N, 14.38.

4.2.18. 2-(3-(4-bromophenyl)-6-oxo-5,6-dihydropyridazin-1(4H)-yl)-N-(thiazol-2-yl)acetamide (SP-17F)

Yield: 61%; mp 169–171 °C; R_f = 0.68; IR (KBr) (cm^{-1}): 3358 (N—H str), 1685 (C═O str), 1598 (C═N str); ^{1}H NMR (400 MHz, DMSO-d_6) δ(ppm): 9.30 (s, 1H, NH), 7.87–7.55 (m, 4H, phenyl), 7.39 (d, J = 7.8, H4-thiazole), 7.24 (d, J = 4.1, H3-thiazole), 3.78 (s, 2H, $-CH_2$), 2.96 (t, J = 7.8, 2H, C$-CH_2$), 2.42 (t, J = 7.8, 2H, CH_2-CO Pyridazinone). ^{13}C NMR (100 MHz, DMSO-d_6) δ (ppm): 168.35, 162.51, 159.68, 145.49, 136.21, 132.27, 130.03, 128.43, 126.02, 112.80, 54.41, 32.30 and 24.38. ESI MS (m/z): 393[M + 1], 394[M + 2]; Anal. Calcd. for $C_{15}H_{13}BrN_4O_2S$: C, 45.81; H, 3.33; N, 14.25; Found: C, 45.83; H, 3.35; N, 14.27.

4.2.19. 2-(6-oxo 3-(thiophen-2-yl)-5,6-dihydropyridazin-1(4H)-yl)-N-(thiazol-2-yl)acetamide (SP-18F)

Yield: 49%; mp 195–197 °C; R_f = 0.56; IR (KBr) (cm^{-1}): 3350 (N—H str), 1680 (C═O str), 1608 (C═N str); ^{1}H NMR (400 MHz, DMSO-d_6) δ(ppm): 9.49 (s, 1H, NH), 7.83–7.51 (m, 3H, thiazole), 7.41 (d, J = 7.2, H4-thiazole), 7.21 (d, J = 4.8, H3-thiazole), 3.82 (s, 2H, $-CH_2$), 2.94 (t, J = 7.8, 2H, C$-CH_2$), 2.48 (t, J = 7.8, 2H, CH_2-CO Pyridazinone). ^{13}C NMR (100 MHz, DMSO-d_6) δ (ppm): 168.41, 162.18, 159.30, 145.71, 136.22, 132.49, 130.19, 128.50, 126.91, 112.52, 54.30, 32.26 and 24.88. ESI MS (m/z): 321[M + 1]; Anal. Calcd. for $C_{13}H_{12}N_4O_2S_2$: C, 48.73; H, 3.78; N, 14.25; Found: C, 48.75; H, 3.79; N, 14.27.

4.3. Pharmacology

All the pharmacological experiments were performed according to ethical principles after Institutional Animal Ethics Committee (IAEC) approval. The investigations were conducted on albino mice of either sex (25–30 g) obtained from central animal house facility, Hamdard University, New Delhi-62 Registration no.173/Go/Re/S/2000CPCSEA. The animals were housed under optimal conditions and allowed free access to standard pellet diet and water (*ad libitum*). The preliminary anticonvulsant (phase I) screening of the test compounds was assessed by following the standard protocols of Antiepileptic Drug Development (ADD) program by NINDS, US using two widely used standard models namely, maximal electroshock seizure (MES), subcutaneous pentylenetetrazole (scPTZ) test and minimal neurological toxicity was evaluated by rotarod test. The most potent compound was also subjected to phase II quantitative determination of ED_{50}, TD_{50}, PI and probit calculations were done by means of computer program Bio Stat 2009 using Finney's method. Hepatotoxicity studies of the compounds were also carried out using procedures described elsewhere. Most active anticonvulsant compounds in phase I screening were also subjected to neuro chemical estimation of GABAs levels in the mice whole brain.

4.4. Maximal electroshock (MES) test

MES test was performed as per the standard protocol [18,19]. The test compounds were dissolved in polyethylene glycol (PEG 400). In the preliminary screening, each compound was administered at three dose levels (30, 100, and 300 mg/kg body mass) and the activity was recorded after 0.5 and 4.0 h intervals of administration. All the animals were administered with the test drug *via i.p*. route. Albino mice were stimulated by using corneal electrodes in which 50 mA current of 60 Hz frequency was applied for 0.25 *sec*. Abolition of hind limb tonic extension spasm was recorded as the end point of test result.

4.5. Subcutaneous pentylenetetrazole (scPTZ) test

The scPTZ test was carried out according to the known protocol [20]. In this method, a 0.5% solution of pentylenetetrazole (75 mg/kg) was utilized subcutaneously in the posterior midline for inducing seizures. The animals were observed for 0.5 h and 4 h. Failure to observe even a threshold seizure (a single episode of clonic spasms of at least 5 s duration) was defined as protection.

4.6. Neurotoxicity-minimal motor impairment

The minimal motor impairment was measured in mice by the rotorod test. The mice were trained to stay on an accelerating rotorod of 3.2 cm diameter rotating at 10 rpm speed. Trained animals were given *i.p.* injection of the test compounds at 30, 100, and 300 mg/kg. Neurotoxicity was observed as the inability of the animal to maintain equilibrium on the rod for at least 1 min in each of the trial done [21].

4.7. Phase II acute toxicity study

The phase I screening was quantified in phase II screening for acute toxicity study (Table 3). Anticonvulsant activity was expressed in terms of the median effective dose (ED_{50}), and neurotoxicity was expressed as the median toxic dose (TD_{50}). For the determination of ED_{50} and TD_{50}values, groups of 10 mice were given a range of intrapeitoneal doses of the test drug until at least three points were established in the range of 10–90% seizure protection or minimal observed neurotoxicity. ED_{50} and TD_{50} values at 95% confidence intervals were calculated by using Probit Analysis program. The time to peak effect of all compounds was determined at the interval of 0.5–4 h range [22,23].

4.8. Serum enzyme activity

For the liver enzyme and total protein estimation, the compounds found active were administered to each animal at a dose of 25 mg/kg/day in methylcellulose for a period of 2 weeks. After the stipulated period, each animal was anaesthetized using anesthetic ether, and blood was collected from the liver to assess the biochemical parameters such as SGOT, SGPT, alkaline phosphate, and total protein according to the reported methods [24–26].

4.9. Gamma-aminobutyric acid estimation

The GABA estimation was performed in brain tissue extract spectrophotometrically after 2 h of drug administration (100 mg/kg, *i.p.*). After dosing, the animals were decapitated and brains were dropped into vials and rinsed with ice-cold isotonic saline followed by homogenization with 0.1 mmol/L phosphate buffer (pH 7.4). The homogenate (10% w/v) was centrifuged at 20000*g* for 30 min and the supernatant so formed was applied on silica gel 60F254 aluminum sheets (10 cm × 10 cm) as stationary phase, using mobile phase comprising water saturated phenol. TLC plates were prewashed with methanol and activated in an oven at 50 °C for 5 min prior to chromatography. The 0.1 mL supernatant solutions were applied on TLC plates in the form of bands. Ascending development to 80 mm was performed in a glass chamber saturated with the mobile phase for 30 min at room temperature. The developed TLC plates were air dried and sprayed with ninhydrin. Ten developed spots were scraped together, mixed with 3 mL distilled water and centrifuged. The supernatant obtained was spectrophotometrically analyzed at 570 nm. The specificity of the method was ascertained by taking standard GABA samples and confirmed by comparing their R_f values. The calibration curve was prepared by plotting OD versus concentration [27,28].

5. Distance mapping

The pharmacophore pattern studies, in which the distance between various groups postulated as essential for anticonvulsant activity was determined from the 3D optimized structures using ACD/3D viewer version 12.01 and Argus Lab 4.0 Mark A. Thompson Planaria Software, LLC. A molecular model was suggested, through conformational analysis of clinically effective, well-known and structurally different anticonvulsant drugs such as a Carbamazepine, Gabapentin, Lamotrigine, Phenytoin, Rufinamide, Diazepam, and Zonisamideon the basis of molecular dynamics distance estimations [29,30].

6. Prediction of ADME properties

A computational study of the title compounds was performed for prediction of ADME properties. Polar surface area (TPSA), miLog P, number of rotatable bonds, molecular volume, and number of hydrogen donor and acceptor atoms and violations of Lipinski's rule of five were calculated by the Molinspiration online property calculation toolkit. The percentage absorption (% ABS) was also calculated by the formula: % ABS = 109-(0.345 - TPSA) [31].

7. Log P determination

The partition coefficient was determined at room temperature using octanol and phosphate buffer mixture. 10 mL of octanol and 10 mL phosphate buffer were mixed and placed in a glass stopper graduated tube. In this mixture, 5 mg of accurately weighed compound was added, followed by shaking with mechanical shaker for 24 h at room temperature. After that, the mixture was transferred to a separating funnel and allowed to dynamically equilibrate for 6 h. The aqueous and octanol phases were separated and filtered through membrane filter. The drug content in aqueous phase was analyzed by UV spectroscopy [32].

8. Docking study

Compound SP-5F was selected as ligand for docking studies with two well-established epilepsy receptors namely $GABA_A$ and Voltage-gated sodium channel receptor by using Maestro 10.5 program (Schrodinger, Inc., USA). These receptors are the most important targets in the design and discovery of successful antiepileptic drugs. The homology model of the diazepam bound $GABA_A$ receptor developed by Richter [33] and Lamotrigine bound Voltage-gated sodium channel by Lipkind and Fozzard [34] was retrieved from the supplementary material of their published paper.

Declaration of Competing Interest

The authors declare no conflict of interest.

Acknowledgement

One of authors, **Sangh Partap** is thankful to University Grants Commission (UGC) New Delhi, India, for financial support. Authors are also thankful to Jamia Hamdard, New Delhi, India for providing facility for the research work.

Appendix A. Supplementary material

Supplementary data to this article can be found online at https://doi.org/10.1016/j.bioorg.2020.103584.

References

[1] S.L. Moshé, E. Perucca, P. Ryvlin, T. Tomson, Epilepsy: new advances, The Lancet 385 (2014) 884–898.
[2] WHO Fact Sheet on Epilepsy - World Health Organization.
[3] R.S. Fisher, M. Parsonage, M. Beaussart, P. Bladin, R. Masland, A.E. Sonnen, et al., Epilepsyand driving: an international perspective. Joint commission on drivers' licensing of the international bureau for epilepsy and the international league against epilepsy, Epilepsia 35 (1994) 675–684.
[4] H. Kaur, B. Kumar, B. Medhi, Antiepileptic drugs in development pipeline: A recent update, eNeurologicalSci 4 (2016) 42–51.
[5] C. Zhuo, R. Jiang, G. Li, M. Shao, Ce Chen, G. Chen, H. Tian, J. Li, R. Xue, D. Jiang, Efficacy and tolerability of second and third generation anti-epileptic drugs in refractory epilepsy: a network meta-analysis, Sci. Rep. 7 (2017) 2535.
[6] L. Dalic, M.J. Cook, Managing drug-resistant epilepsy: challenges and solutions, Neuropsychiatr Dis Treat. 12 (2016) 2605–2616.
[7] M.Z. Hassan, S.A. Khan, M. Amir, Eur. J. Med. Chem. 58 (2012) 206–213.
[8] B. Sharma, A. Verma, U.K. Sharma, S. Prajapati, Efficient synthesis, anticonvulsant and muscle relaxant activities of new 2-((5-amino-1,3,4-thiadiazol2-yl)methyl)-6-phenyl-4,5-dihydropyridazin-3(2H)-one derivatives, Med. Chem. Res. 23 (2014) 146–157.
[9] B. Malawska, A. Scatturin, Application of pharmacophore models for the design and synthesis of new anticonvulsant drugs, Mini. Rev. Med. Chem. 3 (4) (2003 Jun) 341–348.
[10] Mohd. Amir, S. AsifIsrar Ali, Mohd. Zaheen Hassan, Synthesis of benzothiazole derivatives having acetamido and carbothioamidopharmacophore as anticonvulsant agents, Med. Chem. Res. 21 (9) (2012) 2661–2670.
[11] Mohamed F. Zayed, Saleh K. Ihmaid, Hany E.A. Ahmed, Khaled El-Adl, Ahmed M. Asiri, Abdelsattar M. Omar, Synthesis, Modelling, and Anticonvulsant Studies of New Quinazolines Showing Three Highly Active Compounds with Low Toxicity and High Affinity to the GABA-A Receptor, Molecules 22 (2017) 188.
[12] S. Partap, M.S. Yar, M.Z. Hassan, M.J. Akhtar, A.A. Siddiqui, Design, Synthesis, and Pharmacological Screening of Pyridazinone Hybrids as Anticonvulsant Agents, Arch. Pharm. (Weinheim) 350 (10) (2017), https://doi.org/10.1002/ardp.201700135 Epub 2017 Sep 1.
[13] Md. SanghPartap, Jawaid Akhtar, Mohammed Shahar Yar, Mohd Zaheen Hassan, Anees Ahmad Siddiqui, Pyridazinone hybrids: Design, synthesis and evaluation as potential anticonvulsant agents, Bioorg. Chem. 77 (2018) 74–83.
[14] A.A. Siddiqui, R. Mishra, M.S. Yar, Eur. J. Med. Chem. 45 (2010) 2283–2290.
[15] M.S.Y. Khan, A.A. Siddiqui, Indian J. Hetrocyclic Chem. 39B (2000) 614–619.
[16] A.A. Siddiqui, M. Islam, M. Asif, C. Asthana, J. Ultra. Chem. 3 (2007) 176–178.
[17] Raghda R.S. Hussein, Rasha H. Soliman, Ahmed M. Abdelhaleem, Mona H. Ali, Mohamed E.A. Tawfeik, Abdelrahim, Effect of antiepileptic drugs on liver enzymes, Beni-Suef Univ. J. Basic Appl. Sci. 2 (1) (2013) 14–19.
[18] Anticonvulsant Screening Project, Antiepileptic Drug Development Program, National Institute of Health, DHEW Publ (NIH), US, 1978, pp. 78–1093.
[19] L. Krall, J.K. Penry, B.G. White, H.J.E. Kupferberg, A. Swinyard, Epilepsia 19 (1978) 409–428.
[20] E.A. Swinyard, J.H. Woodhead, H.S. White, M.R. Franklin, General principles experimental selection, quantification, and evaluation of anticonvulsants, in: R.H. Levy, R.H. Mattson, B. Melrum, J.K. Penry, F.E. Dreifusseds (Eds.), Antiepileptic Drugs, Raven Press, New York, 1989, pp. 85–102.
[21] N. W. Dunham, T. A. Miya,J. Am. Pharm Assoc. Sci. Ed.1957, 46, 209.
[22] D.J. Finney, Probit Analysis, 3rd ed., Cambridge University Press, London, 1971.
[23] B. Malawska, Curr. Top. Med. Chem. 5 (2005) 85.
[24] J.T. Litchfield, F.A. Wilcoxon, J. Pharmacol. Exp. Ther. 96 (1949) 99–113.
[25] J.G. Reinhold, Standard Methods in Clinical Chemistry, Academic Press, New York, 1953, pp. 88–90.
[26] E.J. King, A.R. Armstrong, Can. Med. Assoc. J. 31 (1934) 381.
[27] V.N. Gokani, M.U. Thakker, J.G. Patel, S.K. Ghosh, S.K. Chatterjee, Ind. J. Physiol. Pharmacol. 23 (1979) 104.
[28] P. Yogeeswari, D. Sriram, R. Thirumurugan, J.V. Raghavendran, K. Sudhan, R.K. Pavana, J. Stables, J. Med. Chem. 48 (2005) 6211.
[29] M.G. Wong, J.A. Defina, P.R. Andrews, J. Med. Chem. 29 (1986) 562.
[30] B.R. Brooks, R.E. Bruccoleri, B.D. Olafson, D.J. States, S. Swaminathan, M. Karplus, J. Comput. Chem. 4 (1983) 217.
[31] P. Ertl, Rohde, B.P. Selzer, J. Med. Chem. 43 (2000) 3717.
[32] A. Vida, V.A. Farrar, M. Ciechanowicz-Rutkowska, J. Grochowski, P. Serda, T. Pilati, G. Filippini, C.N. Hinko, A. El-Assadi, J.A. Moore, I.O. Edafiogho, C.W. Andrews, M. Cory, J.M. Nicholson, K.R. Scott, J. Med. Chem. 36 (1993) 3525.
[33] L. Richter, Nat. Chem. Biol. 8 (2012) 464.
[34] G.M. Lipkind, H.A. Fozzard, Mol. Pharmacol. 78 (2010) 638.